Matrix-Isolation Infrared Spectroscopic and Theoretical Studies on Reactions of Laser-Ablated Germanium Atoms with Water Molecules

Yun-Lei Teng,[†,‡] Ling Jiang,[†,‡] Song Han,[†] and Qiang Xu*,[†,‡]

National Institute of Advanced Industrial Science and Technology (AIST), Ikeda, Osaka 563-8577, Japan, and Graduate School of Science and Technology, Kobe University, Nada Ku, Kobe, Hyogo 657-8501, Japan

Received: March 17, 2007; In Final Form: April 26, 2007

Laser-ablated germanium atoms have been codeposited at 4 K with water molecules in excess argon. Adduct and insertion products, such as $Ge(H_2O)$, HGeOH, HGeO, H_2GeO, GeOH, $Ge(OH)_2$, HGeOGeH, and HGeGeO, have been formed in the present experiments and characterized by using infrared spectroscopy on the basis of the results of the isotopic shifts, mixed isotopic splitting patterns, stepwise annealing, change of reagent concentration and laser energy, and comparison with theoretical predictions. Density functional theory calculations have been performed on these molecules and the corresponding transition states. The agreement between the experimental and calculated vibrational frequencies, relative absorption intensities, and isotopic shifts supports the identification of these molecules from the matrix infrared spectra. Plausible reaction mechanisms have been proposed to account for the formation of these molecules.

Introduction

The interactions of metals with water molecules are of considerable interest from an academic or an industrial viewpoint and have attracted experimental and theoretical attention because of their important roles in a wide variety of areas, such as catalytic synthesis, surface chemistry, and biochemical systems.[1−11] Many efforts have been made to explore the interaction of H_2O with clean and preadsorbed single-crystal metal surfaces and real catalyst surfaces.[1,2] The previous matrix-isolation infrared spectroscopic studies showed that early transition metal atoms reacted with water molecules to form initially the insertion products spontaneously on annealing but the late transition metal atoms reacted with water molecules to form metal−water adducts.[5−9] Recently, it has been found that Nd, Sm, and Eu atoms react with water molecules to form the metal−water adduct complexes and the HMOH insertion molecules in solid argon,[10] but for U and Th, the insertion H_2-UO and H_2ThO molecules are generated.[11]

Much attention has been paid to the interaction of group 14 metal atoms with water. For instance, argon matrix investigations of the reactions of thermally evaporated Si, Ge, Sn, and Pb atoms with water molecules have characterized the $M(H_2O)$, HMOH, HMOH(H_2O), and HM_2OH (M = Si, Ge, Sn, and Pb) complexes.[5a] Furthermore, the electronic absorption spectra of the $M(H_2O)$ (M = Si, Ge, Sn, and Pb) and HMOH (M = Si, Ge, and Sn) complexes have also been observed in the electronic matrix-isolation spectroscopic studies.[5b] In addition, products, such as germylene−water complex (H_2O−GeH_2), germanone (H_2GeO), germanol (H_3GeOH), hydroxygermylene (HGeOH), and germanic acid ($(HO)_2GeO$) were reported in the photochemical reaction of germane and ozone in solid argon.[5d]

Recent investigations on the reactions of laser-ablated metal atoms with small molecules have shown rich chemistry due to

the high reactivities of the ablated metal species.[12,13] Here, we performed a combined matrix-isolation FTIR spectroscopic and theoretical investigation on the reactions of laser-ablated germanium atoms with water molecules in excess argon. IR spectroscopy coupled with theoretical calculations provides evidence for the formation of adduct and insertion molecules, such as $Ge(H_2O)$, HGeOH, HGeO, H_2GeO, GeOH, $Ge(OH)_2$, HGeOGeH, and HGeGeO. In addition, compared with the previous report using thermal sources of germanium,[5a] compounds such as HGeO, H_2GeO, GeOH, $Ge(OH)_2$, and HGeOGeH are observed in the present experiments and are assigned on the basis of the isotopic shifts, mixed isotopic splitting patterns, stepwise annealing, change of reagent concentration and laser energy, and comparison with theoretical predictions.

Experimental and Theoretical Methods

The experiment for laser ablation and matrix-isolation infrared spectroscopy is similar to those previously reported.[13] Briefly, the Nd:YAG laser fundamental (1064 nm, 10 Hz repetition rate with 10 ns pulse width) was focused on the rotating Ge target. The laser-ablated Ge atoms were codeposited with H_2O in excess argon onto a CsI window cooled normally to 4 K by means of a closed-cycle helium refrigerator. Typically, a 1−10 mJ/pulse laser power was used. H_2O, $H_2^{18}O$ (96% ^{18}O), and D_2O were subjected to several freeze−pump−thaw cycles before use. In general, matrix samples were deposited for 30−60 min with a typical rate of 2−4 mmol per hour. After sample deposition, IR spectra were recorded on a BIO-RAD FTS-6000e spectrometer at 0.5 cm^{-1} resolution using a liquid nitrogen cooled HgCdTe (MCT) detector for the spectral range of 5000−400 cm^{-1}. Samples were annealed at different temperatures and subjected to broad-band irradiation ($\lambda > 250$ nm) with use of a high-pressure mercury arc lamp (Ushio, 100 W).

Quantum chemical calculations were performed to predict the structures and vibrational frequencies of the observed reaction products with use of the Gaussian 03 program.[14] The B3LYP density functional method was utilized.[15] The 6-311++G-(d,p) basis set was used for Ge, H, and O atoms. The previous

* Author to whom correspondence should be addressed. E-mail: q.xu@aist.go.jp.
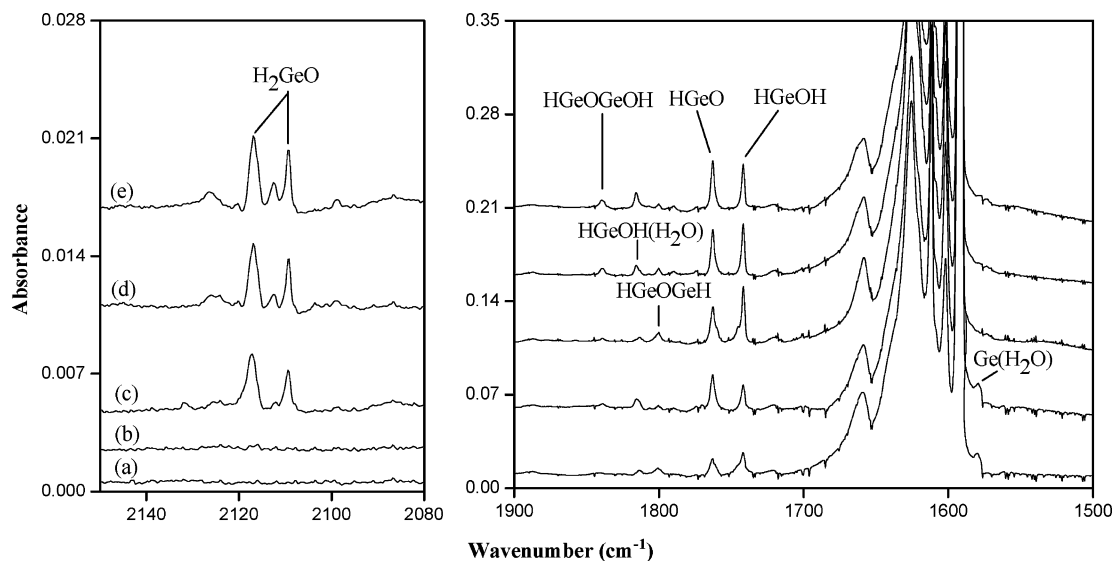† AIST.
‡ Kobe University.

Figure 1. Infrared spectra in the 2150−2080 and 1900−1500 cm^{-1} regions from codeposition of laser-ablated Ge atoms with 1.5% H$_2$O in argon: (a) 1 h sample deposition at 4 K; (b) after annealing to 25 K; (c) after 20 min of broad-band irradiation; (d) after annealing to 30 K; and (e) after annealing to 35 K.

investigations have shown that such computational methods can provide reliable information for the Ge-containing molecules, such as infrared frequencies, relative absorption intensities, and isotopic shifts.[16] Geometries were fully optimized and vibrational frequencies were calculated with analytical second derivatives. Transition-state optimizations were done with the synchronous transit-guided quasi-Newton (STQN) method, followed by the vibtrational calculations showing the obtained structures to be true saddle points. The intrinsic reaction coordinate (IRC) method was used to track minimum energy paths from transition structures to the corresponding local minima.

Results and Discussion

Experiments have been done with H$_2$O concentrations ranging from 0.1% to 2.0% in excess argon. Typical infrared spectra for the reactions of laser-ablated Ge atoms with H$_2$O molecules in excess argon in the selected regions are illustrated in Figures 1−4, and the absorption bands are listed in Table 1. The stepwise annealing and irradiation behavior of these product absorptions are also shown in the figures and will be discussed below.

Quantum chemical calculations have been carried out for the possible isomers and electronic states of the potential product molecules. Figure 5 shows the optimized structures and electronic ground states. Table 2 reports a comparison of the observed and calculated IR frequencies and isotopic frequency ratios of the reaction products. Calculated vibrational frequencies and intensities of the potential products are listed in Table 3.

Ge(H$_2$O). The absorption at 1580.0 cm^{-1} appears during sample deposition, slightly increases on annealing, and disappears after broad-band irradiation (Figure 1). It shifts to 1169.3 cm^{-1} with D$_2$O and to 1571.6 cm^{-1} with H$_2$^{18}O, giving an isotopic H/D ratio of 1.3512 and ^{16}O/^{18}O ratio of 1.0053. The band position and isotopic shifts are characteristics of the H$_2$O bending vibration of a H$_2$O complex perturbed by a metal atom. No intermediate absorptions are observed in the mixed H$_2$^{16}O + H$_2$^{18}O experiments, indicating that only one H$_2$O subunit is involved in this complex. This band is assigned to the H$_2$O bending vibration of the Ge(H$_2$O) complex, which is in agreement with the previous thermal matrix isolation study in solid argon (1577.4 cm^{-1}).[5a]
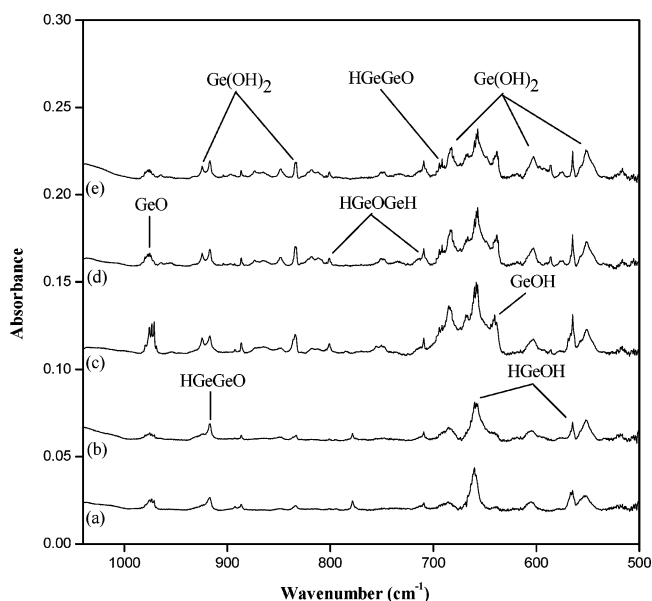

Figure 2. Infrared spectra in the 1040−500 cm^{-1} region from codeposition of laser-ablated Ge atoms with 1.5% H$_2$O in argon: (a) 1 h sample deposition at 4 K; (b) after annealing to 25 K; (c) after 20 min of broad-band irradiation; (d) after annealing to 30 K; and (e) after annealing to 35 K.

Density functional theory (DFT) calculations predict the Ge-(H$_2$O) complex to have an ^{3}A″ electronic ground state with a C_s structure, as shown in Figure 5. The H$_2$O bending vibrational frequency is calculated at 1611.7 cm^{-1} (Table 3), which should be scaled by 0.9803 (observed frequency divided by calculated frequency) to fit the experimental frequency. The calculated isotopic frequency ratios are also in agreement with the experimental values (Table 2).

HGeOH. The absorption at 1741.6 cm^{-1} appears during sample deposition, slightly increases on sample annealing to 25 K, markedly increases on broad-band irradiation, and changes little on further annealing (Figure 1). This band shows a very small shift (2.0 cm^{-1}) with H$_2$^{18}O and shifts to 1258.0 cm^{-1} with D$_2$O. The H/D isotopic ratio of 1.3844 indicates a Ge−H stretching vibrational mode. The spectral feature in the experiment with the H$_2$O/HDO/D$_2$O mixture suggests that only one
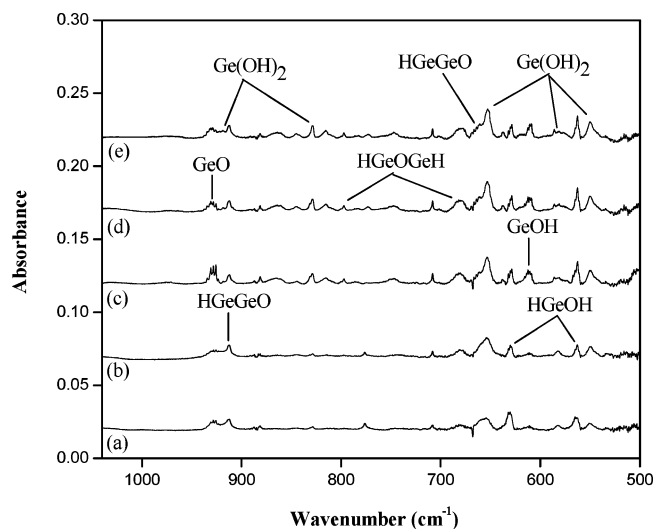
Figure 3. Infrared spectra in the 1050–500 cm^{-1} region from codeposition of laser-ablated Ge atoms with 1.5% $H_2^{18}O$ in argon: (a) 1 h sample deposition at 4 K; (b) after annealing to 25 K; (c) after 20 min of broad-band irradiation; (d) after annealing to 30 K; and (e) after annealing to 35 K.

Figure 4. Infrared spectra in the 750–550 cm^{-1} region from codeposition of laser-ablated Ge atoms with 1.5% D_2O in argon: (a) 1 h sample deposition at 4 K; (b) after annealing to 25 K; (c) after 20 min of broad-band irradiation; (d) after annealing to 30 K; and (e) after annealing to 35 K.
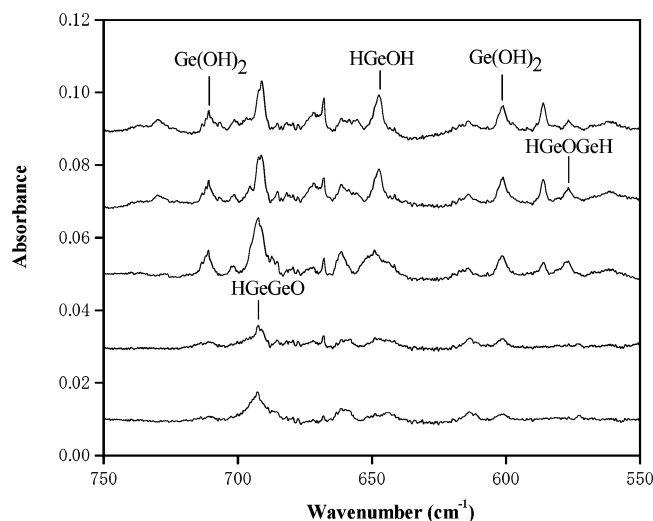
GeH subunit is involved. This band is assigned to the Ge–H stretching vibration of the HGeOH molecule, which is in accord with the previous reports (1741.3[5a] and 1741.1[5d] cm^{-1}). Two bands at 658.4 and 564.7 cm^{-1} exhibit the same annealing and irradiation behavior with the 1741.6 cm^{-1} band, suggesting that these absorptions are due to the different modes of the same molecule. The band at 658.4 cm^{-1} shifts to 630.2 cm^{-1} with $H_2^{18}O$ and to 647.6 cm^{-1} with D_2O, implying a Ge–OH stretching mode is involed. The mixed $H_2^{16}O + H_2^{18}O$ isotopic spectra indicate that only one O atom is involved. On the other hand, the band at 564.7 cm^{-1} slightly shifts with $H_2^{18}O$ and is mainly due to a Ge–O–H deforming mode.

Present DFT calculations predict the HGeOH to have an $^1A'$ electronic ground state with a C_s symmetry (Figure 5) and it is the most stable structural isomer of Ge–H_2O. The Ge–H and Ge–OH stretching vibrations and the Ge–O–H deforming vibration are calculated at 1782.1, 633.2, and 599.7 cm^{-1} (Tables 2 and 3), respectively, which supports the above assignment.

Furthermore, as shown in Table 2, the calculated isotopic frequency ratios are also consistent with the experimental values.

HGeO. The 1762.9 cm^{-1} band appears during sample deposition, visibly increases on sample annealing to 25 K, changes little on broad-band irradiation, and slightly increases on further annealing (Figure 1). This band shows a negligible shift (0.3 cm^{-1}) with $H_2^{18}O$, but shifts to 1274.5 cm^{-1} with D_2O. The isotopic frequency ratios suggest that this band is due to a Ge–H stretching vibrational mode. The mixed $H_2O + HDO + D_2O$ experiments indicate that only one H atom is involved in this mode. Accordingly, it is reasonable to assign the 1762.9 cm^{-1} band to the Ge–H stretching vibration of the HGeO molecule. The HGeO molecule is predicted to have an $^2A'$ ground state with a C_s symmetry (Figure 5). The Ge–H and Ge–O stretching vibrations are predicted at 1735.8 (91) and 840.3 (10 km/mol) cm^{-1}, respectively. The calculated intensity of the Ge–O stretching vibration is too small to be observed, which is consistent with the present experiments.

H_2GeO. The absorptions at 2116.8 and 2109.4 cm^{-1} appear after broad-band irradiation and increase after sample annealing to 30 and 35 K (Figure 1). These two bands exhibit very small shifts (0.5 and 0.1 cm^{-1}) with $H_2^{18}O$ and are assigned to the asymmetric and symmetric Ge–H stretching vibrations of the H_2GeO molecule. The absorption of the D_2GeO species has been overlapped by that of HDO. In the experiment with the $H_2O/HDO/D_2O$ mixture, an additional band at 2114.4 cm^{-1} is observed, indicating that two equivalent H atoms are involved. The band at 953.8 cm^{-1} tracks with the 2116.8 and 2109.4 cm^{-1} bands, suggesting a different mode of the same molecule. This band slightly shifts with D_2O and is due to the Ge–O stretching vibration of the H_2GeO molecule. It is reasonable to assign the three bands to the H_2GeO molecule. In contrast, two weak bands at 2079.6 and 2076.6 cm^{-1} were observed in the reaction of germane with ozone, which were assigned to the H_2GeO molecule, while no experimental data with the H/D isotopic mixture were available.[5d] It is noted that a close band at 2078.7 cm^{-1} due to Ge_2H_6 was observed in the Ge + H_2 experiments.[17]

The present DFT calculations lend support for the assignment of H_2GeO. The H_2GeO molecule is predicted to have an $^1A_1$ ground state with a C_{2v} symmetry. In contrast, the H_2MO (M = Ti, Zr, Hf, and U) molecules have the nonplanar geometry.[8b,11b] The H_2GeO isomer lies 29.4 kcal/mol higher in energy than the most stable isomer HGeOH, and 6.1 kcal/mol lower in energy than Ge(H_2O). The antisymmetric and symmetric Ge–H stretching vibrations are predicted to be 2095.1 and 2085.6 cm^{-1}, respectively, which are in agreement with the experimental values. The Ge–O stretching vibration is calculated at 948.5 cm^{-1}, which is also in accord with the experimental value.

GeOH. A weak absorption at 638.5 cm^{-1} appears during sample deposition, slightly increases after annealing, markedly increases upon broad-band irradiation, and slightly decreases on further annealing (Figure 2). This band shifts to 612.3 cm^{-1} with $H_2^{18}O$. The $^{16}O/^{18}O$ isotopic frequency ratio is 1.0428, implying a Ge–OH stretching vibrational mode. In the mixed $H_2^{16}O + H_2^{18}O$ experiment, only the sum of pure isotopic bands is observed. Accordingly, it is reasonable to assign the 638.5 cm^{-1} band to the Ge–OH stretching vibration of the GeOH molecule, in contrast with the tentative assignment in the previous report on the reactions of germane and oxygen atoms (675.7, 677.4, and 679.1 cm^{-1}).[5d]

B3LYP calculations predict that the GeOH molecule has an $^2A'$ ground state with a nonlinear structure. The doublet GeOH isomer lies 29.3 kcal/mol lower in energy than the HGeO isomer. The calculated Ge–OH stretching vibrational frequency

TABLE 1: Infrared Absorptions (cm^{-1}) from Codeposition of Laser-Ablated Ge Atoms with H$_2$O in Excess Argon at 4 K

H$_2$O	D$_2$O	H$_2{}^{18}$O	H/D	^{16}O/^{18}O	assignment
2116.8		2117.3		0.9998	H$_2$GeO (asy Ge−H stretch)
2109.4		2109.3		1.0000	H$_2$GeO (sym Ge−H stretch)
1839.0	1336.9	1839.1	1.3756	0.9999	HGeOGeOH (Ge−H stretch)
1815.4	1312.6	1815.4	1.3831	1.0000	HGeOH(H$_2$O) (Ge−H stretch)
1800.2	1302.6	1800.0	1.3820	1.0001	HGeOGeH (sym Ge−H stretch)
1762.9	1274.5	1762.6	1.3832	1.0002	HGeO (Ge−H stretch)
1741.6	1258.0	1739.6	1.3844	1.0011	HGeOH (Ge−H stretch)
1580.0	1169.3	1571.6	1.3512	1.0053	Ge(H$_2$O) (H$_2$O bend)
975.9		928.4		1.0512	GeO (Ge−O stretch)
953.8	952.6		1.0013		H$_2$GeO (Ge−O stretch)
924.2	711.0	918.6	1.2999	1.0061	Ge(OH)$_2$ (Ge−O$_B$−H$_B$ bend)
917.1	692.4	912.6	1.3245	1.0049	HGeGeO (asym Ge−H−Ge stretch)
834.2	602.5	829.0	1.3846	1.0063	Ge(OH)$_2$ (Ge−O$_A$−H$_A$ bend)
800.9	576.7	797.1	1.3888	1.0048	HGeOGeH (asy Ge−O−Ge stretch^a)
709.3		681.7		1.0402	HGeOGeH (asym Ge−O−Ge stretch^b)
692.7		664.1		1.0430	HGeGeO (sym Ge−O−Ge stretch)
685.0		653.2		1.0487	Ge(OH)$_2$ (Ge−O$_B$H$_B$ stretch)
658.4	647.6	630.2	1.0167	1.0447	HGeOH (Ge−OH stretch)
638.5		612.3		1.0428	GeOH (Ge−OH stretch)
603.0		581.2		1.0375	Ge(OH)$_2$ (Ge−O$_A$H$_A$ stretch)
564.7		562.8		1.0034	HGeOH (Ge−O−H deform)
550.5		548.4		1.0039	Ge(OH)$_2$ (Ge−O−H deformy)

^{a} Accompanied by Ge−H reverse-phase in-plane wagging. ^{b} Accompanied by Ge−H in-phase in-plane wagging.
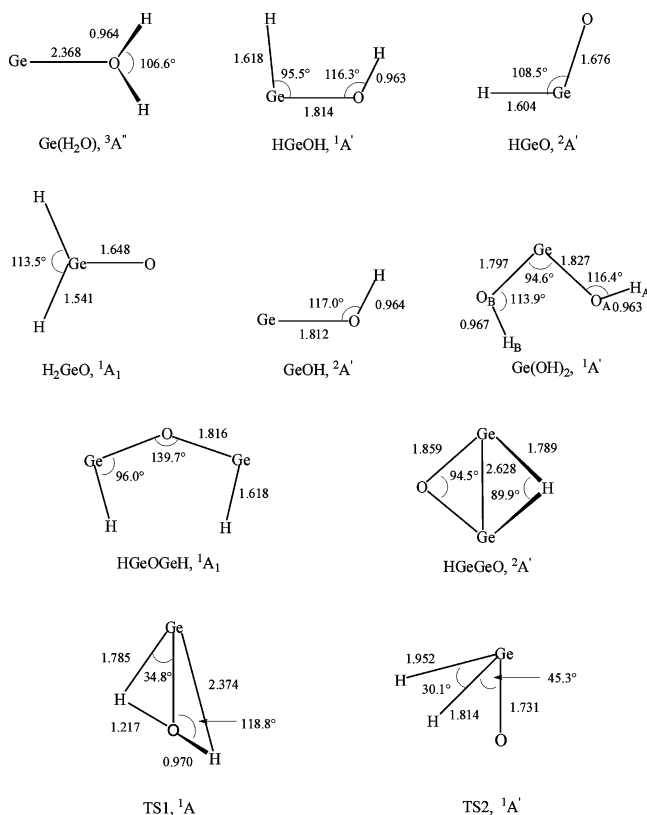

Figure 5. Optimized structures (bond length in angstrom, bond angle in degree) of the possible products and the transition states calculated at the B3LYP level.

and ^{16}O/^{18}O isotopic frequency ratio are 630.1 cm^{-1} and 1.0484 (Table 2), respectively, which are in accord with the experimental observations (638.5 cm^{-1} and 1.0428).

Ge(OH)$_2$. The absorptions at 924.2, 834.2, 685.0, 603.0, and 550.5 cm^{-1} weakly appear during sample deposition, change little after annealing, visibly increase after broad-band irradiation, and change little upon further annealing (Figure 2). The bands at 924.2 and 834.2 cm^{-1} shift to 711.0 and 602.5 cm^{-1} with D$_2$O and to 918.6 and 829.0 cm^{-1} with H$_2{}^{18}$O, respectively, giving the H/D and ^{16}O/^{18}O isotopic frequency ratios of 1.2999,

1.3846 and 1.0061, 1.0063. The 550.5 cm^{-1} band shifts to 548.4 cm^{-1} with H$_2{}^{18}$O. The absorptions at 685.0 and 603.0 cm^{-1} shift to 653.2 and 581.2 cm^{-1} with H$_2{}^{18}$O, giving the ^{16}O/^{18}O isotopic frequency ratios of 1.0487 and 1.0375, which are characteristics of the Ge−OH stretching modes. Accordingly, it is reasonable to assign the absorptions at 924.2, 834.2, 685.0, 603.0, and 550.5 cm^{-1} to the Ge(OH)$_2$ molecule. The analogous M(OH)$_2$ (M = Sn and Pb) molecules have been formed from the M + H$_2$O$_2$ reactions in solid argon.[18]

The Ge(OH)$_2$ molecule is calculated to have an ^{1}A′ ground state with a C_s symmetry (Figure 5), which is 2.1 kcal/mol lower in energy than the one with a C_{2v} symmetry. The Ge−O$_B$H$_B$ and Ge−O$_A$H$_A$ stretching vibrations are calculated at 658.6 and 609.3 cm^{-1}, respectively. As listed in Table 2, the calculated vibrational frequencies and isotopic frequency ratios are consistent with the experimental values, which supports the identification of the Ge(OH)$_2$ molecule from the matrix IR spectra.

HGeOGeH. Three weak absorptions at 1800.2, 800.9, and 709.3 cm^{-1} appear during sample deposition, change little after annealing to 25 K, increase upon broad-band irradiation, and change little after further annealing (Figures 1 and 2). The 1800.2 cm^{-1} band does not shift with H$_2{}^{18}$O but shifts to 1302.6 cm^{-1} with D$_2$O, indicating that the upper mode is due to a Ge−H stretching vibration. The absorptions at 800.9 and 709.3 cm^{-1} shift to 797.1 and 681.7 cm^{-1} with H$_2{}^{18}$O, respectively. Note that these bands are favored under the experimental conditions of higher laser power, suggesting that more than one Ge atom is involved. Accordingly, it is reasonable to assign the absorption at 1800.2 cm^{-1} to a Ge−H stretching vibration and the absorptions at 800.9 and 709.3 cm^{-1} to Ge−O−Ge stretching vibrations coupled with Ge−H vibrations of the HGeOGeH molecule.

The assignment is supported by DFT calculations. As shown in Figure 5, the HGeOGeH molecule is calculated to have an ^{1}A$_1$ ground state. The symmetric Ge−H stretching, the asymmetric Ge−O−Ge stretching accompanied by Ge−H reverse-phase in-plane wagging, and the asymmetric Ge−O−Ge stretching accompanied by Ge−H in-phase in-plane wagging vibrations are predicted to be 1817.7, 773.4, and 747.6 cm^{-1},

Reactions of Laser-Ablated Ge Atoms with H$_2$O

J. Phys. Chem. A, Vol. 111, No. 28, 2007 **6229**

TABLE 2: Comparison of Observed and Calculated IR Frequencies (cm^{-1}) and Isotopic Frequency Ratios of the Reaction Products

molecule	mode	freq		H/D		^{16}O/^{18}O	
		obsd	calcd	obsd	calcd	obsd	calcd
Ge(H$_2$O)	H$_2$O bend	1580.0	1611.7	1.3512	1.3650	1.0053	1.0042
HGeOH	Ge−H stretch	1741.6	1782.1	1.3844	1.4039	1.0011	1.0000
	Ge−OH stretch	658.4	633.2	1.0167	1.0167	1.0447	1.0471
	Ge−O−H deform	564.7	599.7		1.3599	1.0034	1.0042
HGeO	Ge−H stretch	1762.9	1735.8	1.3832	1.4046	1.0002	1.0011
H$_2$GeO	asym Ge−H stretch	2116.8	2095.1		1.4009	0.9998	1.0000
	sym Ge−H stretch	2109.4	2085.6		1.4084	1.0000	1.0000
	Ge−O stretch	953.8	948.5	1.0013	1.0014		1.0492
GeOH	Ge−OH stretch	638.5	630.1		1.0045	1.0428	1.0484
Ge(OH)$_2$	Ge−OB−HB bend	924.2	841.6	1.2999	1.3008	1.0061	1.0065
	Ge−OA−HA bend	834.2	781.4	1.3846	1.3951	1.0063	1.0055
	Ge−OBHB stretch	685.0	658.6		0.9935	1.0487	1.0481
	Ge−OAHA stretch	603.0	609.3		1.0136	1.0375	1.0471
	Ge−O−H deform	550.5	509.3		1.3413	1.0039	1.0057
HGeOGeH	sym Ge−H stretch	1800.2	1817.6	1.3820	1.4044	1.0001	1.0001
	asym Ge−O−Ge stretch^a	800.9	773.4	1.3888	1.4304	1.0048	1.0148
	asym Ge−O−Ge stretch^b	709.3	747.6		1.3827	1.0402	1.0382
HGeGeO	asym Ge−H−Ge stretch	917.1	999.6	1.3245	1.3979	1.0049	1.0004
	sym Ge−O−Ge stretch	692.7	630.9		1.0043	1.0430	1.0505

^{a} Accompanied by Ge−H reverse-phase in-plane wagging. ^{b} Accompanied by Ge−H in-phase in-plane wagging.

TABLE 3: Calculated Vibrational Frequencies (cm^{-1}) and Intensities (km/mol) of Possible Species Involved in the Ge + H$_2$O Reaction (Only the Frequencies above 400 cm^{-1} Are Listed)

species	elec state	point group	frequency (intensity, mode)
Ge(H$_2$O)	^{3}A″	C_s	3896.3 (132, A″), 3794.2 (80, A′), 1611.7 (80, A′), 425.7 (2.2, A″)
HGeOH	^{1}A′	C_s	3849.8 (70, A′), 1782.1 (505, A′), 893.7 (32, A′), 703.5 (46, A′), 633.2 (146, A′), 599.7 (161, A″)
HGeO	^{2}A′	C_s	1735.8 (91, A′), 840.3 (10, A′), 416.4 (17, A′)
H$_2$GeO	^{1}A$_1$	C_{2v}	2095.1 (162, B$_2$), 2085.6 (37, A$_1$), 948.5 (40, A$_1$), 873.2 (70, A$_1$), 575.8 (20, B$_1$), 565.6 (46, B$_2$)
GeOH	^{2}A′	C_s	3824.7 (98, A′), 756.4 (62, A′), 630.1 (137, A′)
Ge(OH)$_2$	^{1}A′	C_s	3851.6 (73, A′), 3798.9 (58, A′), 841.6 (70, A′), 781.4 (105, A′), 658.6 (101, A′), 609.3 (132, A′), 509.3 (83, A″), 414.6 (184, A″)
HGeOGeH	^{1}A$_1$	C_{2v}	1817.7 (677, A$_1$), 1787.5 (31, B$_2$), 786.3 (12, A$_1$), 773.4 (136, B$_2$), 747.6 (445, B$_2$)
HGeGeO	^{2}A′	C_s	1325.9 (50, A′), 999.6 (89, A″), 630.9 (73, A′)
GeO	$^1\Sigma^+$	$C_{\infty v}$	975.3 (66, σ)
TS1	^{1}A	C_1	3719.1 (25, A), 1625.4 (96, A), 742.8 (55, A), 561.2 (33, A), 347.0 (197, A), 1514.4i (1945, A)
TS2	^{1}A′	C_s	1827.3 (78, A′), 1649.1 (221, A′), 1151.8 (32, A″), 817.2 (125, A′), 760.6 (331, A′), 1927.7i (650, A′)

respectively, consistent with the observed values (1800.2, 800.9, and 709.3 cm^{-1}).

HGeGeO. Two absorptions at 917.1 and 692.7 cm^{-1} appear during sample deposition and change little after annealing and broad-band irradiation (Figure 2). The 917.1 cm^{-1} band shifts to 912.6 cm^{-1} with H$_2$^{18}O and to 692.4 cm^{-1} with D$_2$O, giving an isotopic ^{16}O/^{18}O ratio of 1.0049 and an H/D ratio of 1.3245. The band position and isotopic ratios of the 917.1 cm^{-1} band indicate that this absorption is due to a Ge−H stretching vibration. The 692.7 cm^{-1} band shifts to 664.1 cm^{-1} with H$_2$^{18}O, showing an isotopic ^{16}O/^{18}O ratio of 1.0430. This suggests a Ge−O stretching vibration. Accordingly, it is reasonable to assign the 917.1 and 692.7 cm^{-1} bands to the Ge−H stretching and Ge−O stretching vibrations of the HGeGeO molecule, in contrast with the previous report (784.8, 710.8, and 683.0 cm^{-1}).[5a]

B3LYP calculations predict that the HGeGeO molecule has a cyclic structure with an ^{2}A′ ground state and a C_s symmetry (Figure 5). The calculated asymmetric Ge−H−Ge stretching and symmetric Ge−O−Ge stretching vibrations are 999.6 and 630.9 cm^{-1}, respectively, in agreement with the experimental observation.

Other Absorptions. An absorption at 1839.0 cm^{-1} appears during sample deposition, changes little after annealing to 25 K and broad-band irradiation, and slightly increases upon further annealing (Figure 1). This band is favored with higher laser energy, indicating that more than one Ge atom is involved. This

band is tentatively assigned to the Ge−H stretching vibration of the HGeOGeOH molecule. A weak absorption at 1815.4 cm^{-1} appears during sample deposition, increases on annealing, decreases after broad-band irradiation, and increases on further annealing (Figure 1), which is favored with higher water concentration. This band is tentatively assigned to the Ge−H stretching vibration of the HGeOH(H$_2$O) molecule based on the band position and changes of reagent concentration, annealing, and irradiation.

Reaction Mechanism. On the basis of the behavior of sample annealing and irradiation together with the observed species and calculated stable isomers, plausible reaction mechanisms can be proposed as follows. Under the present experimental conditions, laser-ablated Ge atoms codeposit with water molecules to form the Ge(H$_2$O) complex during sample deposition (Figure 1), which slightly increases on annealing, suggesting that the ground state ^{3}P Ge atoms can react with water to form the Ge-(H$_2$O) complex spontaneously. This addition reaction is predicted to be exothermic by about 10.4 kcal/mol (reaction 1). The IR absorptions of HGeOH appear during sample deposition and increase upon broad-band irradiation while the IR absorption of Ge(H$_2$O) disappears, implying that the HGeOH molecule may be generated from the isomerization of Ge(H$_2$O) (reaction 2) via irradiation in the laser ablation plume during sample deposition and upon broad-band irradiation. This isomerization is exothermic (−35.5 kcal/mol) and the activation barrier is predicted to be 32.8 kcal/mol (Figure 6), which can be obtained
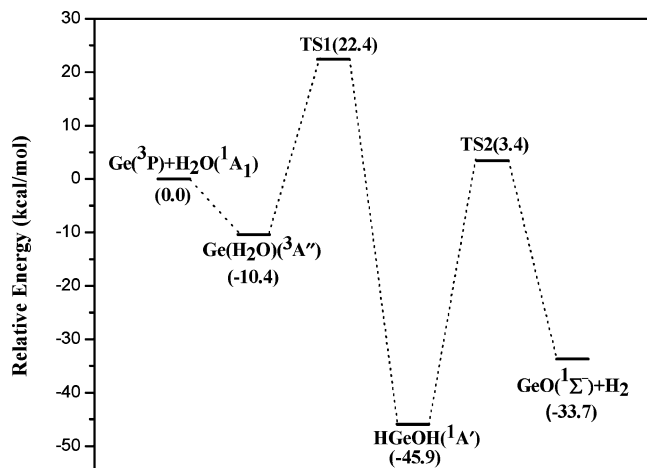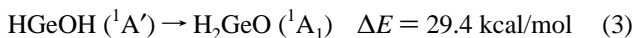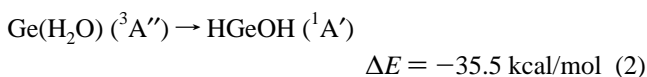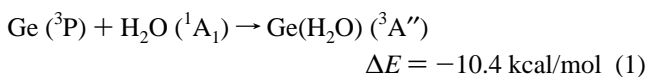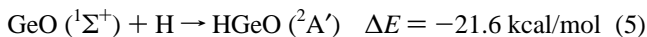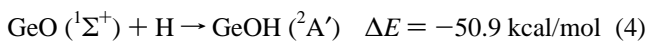
Figure 6. Potential energy surface for the Ge + H$_2$O reactions calculated at the B3LYP level. Energies given are in kcal/mol and are relative to the separated ground-state reactants: Ge (^{3}P) + H$_2$O (^{1}A$_1$).
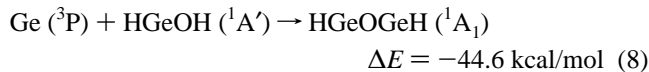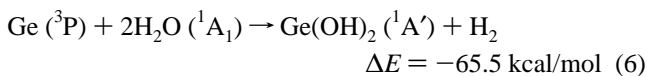
by ultraviolet−visible irradiation. It is also noted that the H$_2$-GeO molecule appears after broad-band irradiation, which may be formed from the isomerization of the HGeOH molecule (reaction 3, 29.4 kcal/mol).

$$\text{Ge }(^3\text{P}) + \text{H}_2\text{O }(^1\text{A}_1) \rightarrow \text{Ge(H}_2\text{O)} (^3\text{A}'')$$
$$\Delta E = -10.4 \text{ kcal/mol} \quad (1)$$

$$\text{Ge(H}_2\text{O)} (^3\text{A}'') \rightarrow \text{HGeOH }(^1\text{A}')$$
$$\Delta E = -35.5 \text{ kcal/mol} \quad (2)$$

$$\text{HGeOH }(^1\text{A}') \rightarrow \text{H}_2\text{GeO }(^1\text{A}_1) \quad \Delta E = 29.4 \text{ kcal/mol} \quad (3)$$

It can be seen from Figures 1 and 2 that the IR absorptions of HGeO and GeO appear during sample deposition, suggesting that a portion of the Ge(H$_2$O) and HGeOH complexes formed during the codeposition of H$_2$O with the Ge atoms generated by pulse laser ablation are dissociated to HGeO, GeO, H, or H$_2$ during deposition. The formation of these molecules may be due to the reactions of excited atoms which are produced during laser ablation of the metal target. Similar features have also been observed in the reactions of group 4 metal atoms with H$_2$O in solid argon.[8b] Then, the GeO molecule may react with the H atom to produce GeOH or HGeO (reactions 4 and 5).

$$\text{GeO }(^1\Sigma^+) + \text{H} \rightarrow \text{GeOH }(^2\text{A}') \quad \Delta E = -50.9 \text{ kcal/mol} \quad (4)$$

$$\text{GeO }(^1\Sigma^+) + \text{H} \rightarrow \text{HGeO }(^2\text{A}') \quad \Delta E = -21.6 \text{ kcal/mol} \quad (5)$$

The Ge(OH)$_2$ molecule appears during sample deposition, and increases upon annealing, which may be formed by the reaction of the Ge atom with two water molecules (reaction 6), suggesting that the formation of the Ge(OH)$_2$ molecule does not require activation energy. Reaction 6 is predicted to be exothermic (−65.5 kcal/mol). The HGeGeO molecule is generated during sample deposition by using high laser power, which is probably formed by the reaction of a Ge atom with the HGeO molecule (reaction 7, −84.3 kcal/mol). Similarly, the HGeOGeH molecule may be generated via the addition of a Ge atom to the HGeOH molecule (reaction 8).

$$\text{Ge }(^3\text{P}) + 2\text{H}_2\text{O }(^1\text{A}_1) \rightarrow \text{Ge(OH)}_2 (^1\text{A}') + \text{H}_2$$
$$\Delta E = -65.5 \text{ kcal/mol} \quad (6)$$

$$\text{Ge }(^3\text{P}) + \text{HGeO }(^1\text{A}') \rightarrow \text{HGeGeO }(^2\text{A}')$$
$$\Delta E = -84.3 \text{ kcal/mol} \quad (7)$$

$$\text{Ge }(^3\text{P}) + \text{HGeOH }(^1\text{A}') \rightarrow \text{HGeOGeH }(^1\text{A}_1)$$
$$\Delta E = -44.6 \text{ kcal/mol} \quad (8)$$

Conclusions

Reactions of laser-ablated germanium atoms with water molecules in excess argon have been studied by using matrix-isolation infrared spectroscopy. Adduct and insertion products, such as Ge(H$_2$O), HGeOH, HGeO, H$_2$GeO, GeOH, Ge(OH)$_2$, HGeOGeH, and HGeGeO, are observed in the present experiments. The products are assigned on the basis of the results of the isotopic substitution, stepwise annealing, change of water concentration and laser energy, and comparison with theoretical predictions. The Ge(H$_2$O) molecule rearranges to the HGeOH molecule, which further isomerizes to the H$_2$GeO molecule upon broad-band irradiation. The Ge(OH)$_2$ molecule is formed by the reaction of the Ge atom with two water molecules. Energetic analysis for the possible reactions of Ge atoms with H$_2$O molecules has also been given.

References and Notes

(1) Thiel, P. A.; Madey, T. E. *Surf. Sci. Rep.* **1987**, *7*, 211.
(2) Henderson, M. A. *Surf. Sci. Rep.* **1998**, *46*, 1.
(3) Kovalenko, A.; Hirata, F. *J. Chem. Phys.* **1999**, *110*, 10095.
(4) (a) Guo, B. C.; Kerns, K. P.; Castleman, A. W. *J. Phys. Chem.* **1992**, *96*, 4879. (b) Tilson, J. L.; Harrison, J. F. *J. Phys. Chem.* **1991**, *95*, 5097. (c) Chen, Y. M.; Clemmer, D. E.; Armentrout, P. B. *J. Phys. Chem.* **1994**, *98*, 11490. (d) Liu, K.; Parson, J. M. *J. Chem. Phys.* **1978**, *68*, 1794.
(5) (a) Kauffman, J. W.; Hauge, R. H.; Margrave, J. L. *ACS Symp. Ser.* **1982**, *179*, 355. (b) Douglas, M. A.; Hauge, R. H.; Margrave, J. L. *High Temp. Sci.* **1986**, *22*, 47. (c) Ismail, Z. K.; Hauge, R. H.; Fredin, L.; Kauffman, J. W.; Margrave, J. L. *J. Chem. Phys.* **1982**, *77*, 1617. (d) Withnall, R.; Andrews, L. *J. Phys. Chem.* **1990**, *94*, 2351.
(6) (a) Kauffman, J. W.; Hauge, R. H.; Margrave, J. L. *J. Phys. Chem.* **1985**, *89*, 3541. (b) Kauffman, J. W.; Hauge, R. H.; Margrave, J. L. *J. Phys. Chem.* **1985**, *89*, 3547.
(7) (a) Zhang, L. N.; Dong, J.; Zhou, M. F. *J. Phys. Chem. A* **2000**, *104*, 8882. (b) Zhang, L. N.; Shao, L. M.; Zhou, M. F. *Chem. Phys.* **2001**, *272*, 27.
(8) (a) Zhou, M. F.; Dong, J.; Zhang, L. N.; Qin, Q. Z. *J. Am. Chem. Soc.* **2001**, *123*, 135. (b) Zhou, M. F.; Zhang, L. N.; Dong, J.; Qin, Q. Z. *J. Am. Chem. Soc.* **2000**, *122*, 10680.
(9) (a) Zhou, M. F.; Zhang, L. N.; Shao, L. M.; Wang, W. N.; Fan, K. N.; Qin, Q. Z. *J. Phys. Chem. A* **2001**, *105*, 5801. (b) Zhang, L. N.; Zhou, M. F.; Shao, L. M.; Wang, W. N.; Fan, K. N.; Qin, Q. Z. *J. Phys. Chem. A* **2001**, *105*, 6998.
(10) Xu, J.; Zhou, M. F. *J. Phys. Chem. A* **2006**, *110*, 10575.
(11) (a) Liang, B. Y.; Andrews, L.; Li, J.; Bursten, B. E. *J. Am. Chem. Soc.* **2002**, *124*, 6723. (b) Liang, B. Y.; Hunt, R. D.; Kushto, G. P.; Andrews, L.; Li, J.; Bursten, B. E. *Inorg. Chem.* **2005**, *44*, 2159.
(12) (a) Zhou, M. F.; Andrews, L.; Bauschlicher, C. W., Jr. *Chem. Rev.* **2001**, *101*, 1931. (b) Himmel, H. J.; Downs, A. J.; Greene, T. M. *Chem. Rev.* **2002**, *102*, 4191 and references cited therein.
(13) (a) Burkholder, T. R.; Andrews, L. *J. Chem. Phys.* **1991**, *95*, 8697. (b) Zhou, M. F.; Tsumori, N.; Andrews, L.; Xu, Q. *J. Phys. Chem. A* **2003**, *107*, 2458. (c) Jiang, L.; Xu, Q. *J. Chem. Phys.* **2005**, *122*, 034505. (d) Jiang, L.; Xu, Q. *J. Am. Chem. Soc.* **2005**, *127*, 42. (e) Jiang, L.; Xu, Q. *J. Am. Chem. Soc.* **2005**, *127*, 8906. (f) Xu, Q.; Jiang, L.; Tsumori, N. *Angew. Chem., Int. Ed.* **2005**, *44*, 4338.
(14) Frisch, M. J.; Trucks, G. W.; Schlegel, H. B.; Scuseria, G. E.; Robb, M. A.; Cheeseman, J. R.; Montgomery, J. A., Jr.; Vreven, T.; Kudin, K. N.; Burant, J. C.; Millam, J. M.; Iyengar, S. S.; Tomasi, J.; Barone, V.; Mennucci, B.; Cossi, M.; Scalmani, G.; Rega, N.; Petersson, G. A.; Nakatsuji, H.; Hada, M.; Ehara, M.; Toyota, K.; Fukuda, R.; Hasegawa, J.;

Ishida, M.; Nakajima, T.; Honda, Y.; Kitao, O.; Nakai, H.; Klene, M.; Li, X.; Knox, J. E.; Hratchian, H. P.; Cross, J. B.; Adamo, C.; Jaramillo, J.; Gomperts, R.; Stratmann, R. E.; Yazyev, O.; Austin, A. J.; Cammi, R.; Pomelli, C.; Ochterski, J. W.; Ayala, P. Y.; Morokuma, K.; Voth, G. A.; Salvador, P.; Dannenberg, J. J.; Zakrzewski, V. G.; Dapprich, S.; Daniels, A. D.; Strain, M. C.; Farkas, O.; Malick, D. K.; Rabuck, A. D.; Raghavachari, K.; Foresman, J. B.; Ortiz, J. V.; Cui, Q.; Baboul, A. G.; Clifford, S.; Cioslowski, J.; Stefanov, B. B.; Liu, G.; Liashenko, A.; Piskorz, P.; Komaromi, I.; Martin, R. L.; Fox, D. J.; Keith, T.; Al-Laham, M. A.; Peng, C. Y.; Nanayakkara, A.; Challacombe, M.; Gill, P. M. W.; Johnson, B.; Chen, W.; Wong, M. W.; Gonzalez, C.; Pople, J. A. *Gaussian 03*, revision B.04; Gaussian, Inc.: Pittsburgh, PA, 2003.

(15) (a) Lee, C.; Yang, E.; Parr, R. G. *Phys. Rev. B* **1988**, *37*, 785. (b) Becke, A. D. *J. Chem. Phys*. **1993**, *98*, 5648.

(16) (a) Zhou, M. F.; Shao, L. M.; Miao, L. *J. Phys. Chem. A* **2002**, *106*, 6483. (b) Zhou, M. F.; Jiang, L.; Xu. Q. *J. Phys. Chem. A* **2005**, *109*, 3325.

(17) Wang, X. F.; Andrews, L. *J. Am. Chem. Soc*. **2003**, *125*, 6581.

(18) Wang, X. F.; Andrews, L. *J. Phys. Chem. A* **2005**, *109*, 9013.